DOI: 10.1002/((please add manuscript number))
Article type: Communication

Boosting photovoltaic output of ferroelectric ceramics by opto-electric control of domains

Yang Bai, Gaurav Vats, Jan Seidel, Heli Jantunen and Jari Juuti

Dr. Y. Bai, Prof. H. Jantunen, Dr. J. Juuti
Microelectronics Research Unit, Faculty of Information Technology and Electrical Engineering, University of Oulu, FI-90580 Oulu, Finland
E-mail: yang.bai@oulu.fi

G. Vats, Prof. J. Seidel
School of Materials Science and Engineering, Faculty of Science, University of New South Wales, Sydney NSW 2052, Australia

Keywords: multi-source energy harvesting, photo-ferroelectric, ceramics, photovoltaic, efficiency boost

Abstract

Photo-ferroelectric single crystals and highly oriented thin-films have been extensively researched recently, with increasing photovoltaic energy conversion efficiency (from 0.5 % up to 8.1 %) achieved. Rare attention has been paid to polycrystalline ceramics, potentially due to their negligible efficiency. However, ceramics offer simple and cost-effective fabrication routes and stable performance compared to single crystals and thin-films. Therefore, a significantly increased efficiency of photo-ferroelectric ceramics contributes towards widened application areas for photo-ferroelectrics, e.g. multi-source energy harvesting. In this paper, all-optical domain control under illumination, visible-range light-tunable photo-diode/transistor phenomena and opto-electrically tunable photovoltaic properties are demonstrated, using a recently discovered photo-ferroelectric ceramic – $(K_{0.49}Na_{0.49}Ba_{0.02})(Nb_{0.99}Ni_{0.01})O_{2.995}$ (KNBNNO). For this monolithic material, tuning of the electric conductivity independent of

ferroelectricity is achieved, which previously could only be achieved in organic phase-separate blends. Guided by these discoveries, a boost of 5 orders of magnitude in the photovoltaic output power and energy conversion efficiency is achieved via optical and electrical control of ferroelectric domains in an energy harvesting circuit. These results provide a new approach and knowledge for other photo-ferroelectrics to further boost their efficiency for energy efficient circuitry designs and enable the development of a wide range of optoelectronic devices.

Photo-ferroelectric materials have been under investigation since the 1970s, and are experiencing extensive research interest.[1-5] Thanks to their non-centrosymmetric microstructure which promotes the desired photo-excited carrier separation, photo-ferroelectrics allow an open-circuit voltage higher than the band gap.[4] To the state of the art, a maximum photovoltaic energy conversion efficiency of 8.1 % has been achieved with a multi-layer Bi_2FeCrO_6 (BFCO) thin-film solar cell.[6] Although this is still far below the most efficient (38.8 %) multi-junction cell made from GaAs thin-films[7], photo-ferroelectrics offer the possibility of exceeding the S-Q (Shockley-Queisser) limit, which is advantageous compared to conventional semiconductor solar cells.[4] In most cases, the band gaps of photo-ferroelectric single crystals or polycrystalline ceramics such as $BaTiO_3$ and $BiFeO_3$ are wider than 2.7 eV. This value is far from the ideal value of 1.34 eV for the optimum S-Q (Shockley-Queisser) limit, making them less likely to effectively absorb the whole visible-range of light in the solar spectrum.[8-10] However, in our previous research[11], the KNBNNO polycrystalline ceramic was able to exhibit a band gap similar to that of the most advanced BFCO thin-film photo-ferroelectrics (1.5-2.7 eV).[6] The KNBNNO's band gap is re-confirmed here (**Figure S1** in Supporting Information), where the sample showed responses to the entire visible range. It was also comparable to the widely studied organic-halide perovskite thin films[12] and the emerging $(KNbO_3)_{1-x}(BaNi_{0.5}Nb_{0.5}O_{3-\delta})_x$ ceramics[8, 13] with > 1.1 eV tunable band gaps. The narrow band

gaps enable absorption of the entire visible light spectrum. Comparing the above materials, KNBNNO has additional interesting properties, i.e. its proven much larger remanent polarization (~ 11.7 μC cm^{-2}) and piezoelectric (d_{33} ~100 pC N^{-1}) and pyroelectric (~128 μC m^{-2} K^{-1}) coefficients.[11] Furthermore, although the efficiencies of photo-ferroelectric and other perovskite solar cells have been significantly improved, they are all achieved with single crystals or highly oriented thin-films. Single crystals and BFCO thin films are known for their fabrication cost/challenge[6, 14], and organic-inorganic perovskite thin films usually suffer from stability issues.[15, 16] As a ceramic, KNBNNO can be fabricated easily and performs stably under illumination (**Figure S2**a in Supporting Information). However, rare attention is paid to the photovoltaic output improvement of photo-ferroelectric ceramics. In fact, it is desirable to replace single crystals with ceramics if the ceramics can achieve the same level of the single crystals' performance. For instance, ultrahigh piezoelectricity has been recently reported in ferroelectric ceramics which are considered promising single crystal substitutes[14]. Therefore, efforts should also be made towards high-performance photo-ferroelectric ceramics. Here, the advantageous KNBNNO ceramic is used to investigate the optical control of ferroelectric domains.

To reveal the strong interaction between illumination and domain wall motion, the ferroelectric hysteresis loops (P-E loops) of the KNBNNO samples were measured under different conditions (**Figure 1**). It should be noted that the loops were measured for the entire surface of the samples (~110 mm^2) while the spot size of the laser illumination on the samples was only 0.5 mm^2. The increase of the remanent polarization under illumination compared to the cases in the dark can be clearly seen (Figure 1a and 1c). It has been reported that similar phenomena were observed in $CH_3NH_3PbI_3$ (organic-inorganic perovskite) thin films, where a 405 nm laser illumination induced an increase in the remanent polarization.[17] However, such an increase was observed in only the first few cycles of the measurement before it disappeared[17], possibly due to either the decay of the thin film or the saturation of the charge carrier separation.[15, 16]

By contrast, the photo-induced increase of the polarization in KNBNNO ceramics has been proven to be constant and reproducible, where loops with the same increase of remanent polarization were obtained in the first 6 cycles of the measurement (Figure S2b in Supporting Information). The observed increase of the remanent polarization in ferroelectrics under illumination could result from either of two reasons – photo-stimulated domain switching or localized heating.[17-20] The latter has been excluded in our case because the temperature dependent P-E loops showed negligible difference in polarization (**Figure S3** in Supporting Information). The mechanisms of the former have been previously discussed, regarding the asymmetric potentials generated at the interfaces between ‘‘a’’ and ‘‘c’’ domains (spontaneous polarizations perpendicular to and in parallel with the external electric field, respectively).[21] With these potentials and light illumination, a net displacement of the locally free charges at the domain walls can be induced, thus unbalancing the pressure on the domain wall and stimulating domain wall motion.[21]

One of the most interesting discoveries was the time dependence of the photo-induced/stimulated domain wall motion. The lower the frequency, the larger was the increase of the remanent polarization under the same illumination. In comparison, the loops measured in the dark showed only a very weak or negligible frequency dependence (**Figure S4**a-b in Supporting Information). This implies that the photo-induced domain poling is time-dependent. The above-mentioned photo-induced charge displacement introduces an additional electric potential, preventing a part of the ‘‘c’’ domains from reversing to become ‘‘a’’ domains when the external electric field disappears, as is the case for poling in the dark.[22] The domains do not switch at the same time and the number of switched domains is time-dependent.[22] Although a similar effect was reported with a highly oriented $(Pb_{0.6}Li_{0.2}Bi_{0.2})(Zr_{0.2}Ti_{0.8})O_3$ (PLBZT) thin film[18], the time dependence could not be concluded as there was already a frequency dependence for the P-E loops, even when measured in the dark. For further evidence, a wide band gap (> 3 eV), $(Ba_{0.85}Ca_{0.15})(Zr_{0.1}Ti_{0.9})O_3$ ceramic reference sample was measured

in the same way. No additional domain switching could be realized (Figure S4c in Supporting Information), indicating true photo-stimulated domain switching shown in Figure 1. The time-dependence can also be proven at the nanoscale, where domain switching with light exposure was observed (**Figure S5** in Supporting Information).

To understand the practical implications of the phenomena presented above, an unpoled KNBNNO sample (with randomly oriented domains) was exposed to white light. The piezoelectric charge coefficient d_{33} was measured before, during and after the exposure. The unpoled KNBNNO sample exhibited a d_{33} of nearly zero. After one hour of exposure under the light, the d_{33} remained unchanged. However, after being exposed overnight (> 8 hours) which allowed sufficient time for optical poling of the domains, a d_{33} of 4 pC/N was obtained at the same measuring point of the sample's surface. Thus, macroscopic poling was achieved solely by normal room light (white light) and in the absence of any externally applied electric field. This proves the existence of photo-induced, permanent domain switching. Accompanying this true poling process with light, a change of the pyroelectric response was observed (**Figure 2**a). An increased pyro-current could be clearly seen for the sample poled under white light compared to the unpoled case.

Due to the different amount of free charge carriers induced by different incident light intensities and wavelengths, it was also possible to tune the conductivity (Figure 2b-d). The most significant change was found with the 405 nm laser, where a conductivity increased more than two orders of magnitude. It is worth noting that the results shown in Figure 1d and Figure 2b-d provide an opportunity to tune the conductivity independent of ferroelectricity in a monolithic material, which previously could only be achieved in organic phase-separate blends.[23]

Light and electric field can be applied simultaneously to promote domain switching and thus improve the d_{33}. In the poling experiments, the same KNBNNO sample poled under illumination (405 nm, 50 mW laser) exhibited a 56 % higher d_{33} value (39 pC/N) than the one poled in the dark (25 pC/N). Both the d_{33} values were measured in the dark. This increase also

resulted from the photo-stimulated domain switching. Meanwhile, a boosted photocurrent can be obtained together with a DC electric field bias. The polarity of the photocurrent was reversible according to the polarity of the bias, even when the sample was poled (**Figure 3**a). A rather small bias field (~ 0.67 kV cm^{-1} compared to the coercive field of > 10 kV cm^{-1}) was able to induce a two orders of magnitude boost to the photocurrent which was completely polarity reversible. The magnitude of the boost was related to the bias field. No lower threshold was observed, i.e. the boosting phenomenon could always been seen even with smaller bias fields. This phenomenon was also observed for the entire visible range, even for an unpoled sample (**Figure S6** in Supporting Information). Both the electric bias and illumination are proven to be compulsory for a current boost, with the absence of either leading to the disappearance of the phenomenon (**Figure S7**a-b in Supporting Information). The photocurrents observed here were shown to be due to the photovoltaic effect, as the relationship between the photocurrent and incident light power was linear (Figure S7c-d in Supporting Information).[24, 25]

Without any electric bias, the photovoltaic performance (current density-voltage (*J*-*V*) curves) was strongly related to the extent of the domain alignment (**Figure 3**b-e). The short-circuit current, maximum output power and photovoltaic energy conversion efficiency were all positively related to the d_{33} (**Table S1** in Supporting Information). For the same material, higher d_{33} induced larger net polarization, i.e. more aligned domains in the poling direction. Therefore, the net polarization plays an important role in the photovoltaic effect for the KNBNNO. The photocurrent dependence on the net polarization could also be observed in KNN doped with different concentrations of $(BaNi_{0.5}Nb_{0.5})O_{2.75}$ (BNNO) (**Figure S8** in Supporting Information). Based on the above findings, i.e. (1) incident light stimulates domain wall motion, (2) higher extent of domain alignment induces larger photovoltaic output and (3) DC bias helps to boost photocurrent, a device comprising a KNBNNO cell, a charged capacitor (100 μF, 18 V as the DC bias) and a resistive load (1 MΩ) connected in series was used to demonstrate the approach

of photo-output boost. **Figure 4** shows the schematic of the circuit and the calculated powers on the resistor. Before the laser was turned on (in the dark), the high resistance (>> 30 MΩ, **Figure S9**a in Supporting Information) of the KNBNNO cell prevented the capacitor from releasing a recognizable current, leading to negligible power on the 1 MΩ resistor. When the laser was turned on illuminating the KNBNNO cell, its resistance rapidly dropped to only 6 MΩ (Figure S9a in Supporting Information), inducing an increasing current in the circuit thus an increasing power on the 1 MΩ resistive load (Figure 4b). Meanwhile, the KNBNNO cell generated a significantly higher power than that given by the capacitor, providing a boosted gross output power on the 1 MΩ resistive load. The net output power was calculated by deducting the power given by the capacitor from the gross power, i.e. representing the output power provided by the KNBNNO cell. As a consequence of the photo-induced domain wall motion, local free charges were extracted by the biasing electric potential. In addition, the DC bias aligned more domains which further elevated the photo-output level. This explanation is supported by the decreasing net power as a function of capacitor voltage (Figure 4b and Figure S9a in Supporting Information). The maximum net output power (~ 60 μW) gives the cell an energy conversion efficiency of 0.12 %, more than 60,000 times larger than that without a DC bias (Table S1 in Supporting Information). This constitutes an increase of 5 orders of magnitude. By exploiting the various interactions between visible light and domains presented above, other optoelectronic applications can also be explored. The boosted photo-output of the KNBNNO cell can provide an approach for other photo-ferroelectrics to further improve their photovoltaic performance. The visible-range optical control of domain switching can open doors for optoferroelectric devices such as photo-actuators and data storage with specific wavelength sensitivities. The reversible photovoltaic effect with electric bias can be used to develop photodiodes and phototransistors. The conductivity change under illumination can induce photo-tunable semiconductors. The KNBNNO provides an opportunity towards the

replacement of photo-ferroelectric single crystals with polycrystalline ceramics, and contributes to energy efficient designs in future ultra-low power circuits.

Experimental Section

Sample fabrication: Ceramic powder with the composition $(K_{0.49}Na_{0.49}Ba_{0.02})(Nb_{0.99}Ni_{0.01})O_{2.995}$ (KNBNNO) was fabricated via the solid state route. The starting reactants of K_2CO_3 (≥ 99 %, J. T. Baker, USA), Na_2CO_3 (≥ 99 %, Sigma-Aldrich, USA), $BaCO_3$ (99.98 %, Aldrich Chemistry, USA), NiO (99.999 %, Aldrich Chemistry, USA) and Nb_2O_5 (99.9 %, Aldrich Chemistry, USA) were weighed according to the stoichiometry of each composition. All of the reactants were dried at 220 ˚C for over 4 hours before weighing, in order to remove the potentially adsorbed water and to give precise weights with 0.01 mg readability and 1 mg accuracy (ES 225SM-DR, Precisa, Dietikon, Switzerland). All of the weighed reactants for each composition were loaded together into a ZrO_2 jar before mixing. The mixing was carried out in the jar with ethanol using a planetary ball mill (Pulverisette 6, Fritsch, Idar-Oberstein, Germany) with ZrO_2 balls (3 mm diameter) for 6 hours, followed by drying at 80 ˚C. The mixed powder was subjected to a one-step calcination at 850 ˚C for 4 hours in air prior to further planetary ball milling for 12 hours with ZrO_2 balls and ethanol. The milled and dried (at 80 ˚C) powder was then mixed with 8.8 wt.% of binder (3.3 wt.% polyvinyl alcohol dissolved in deionized water), and uniaxially pressed at 62 MPa into disc-shaped green bodies with a diameter of 14.5 mm. The binders in the green bodies were burnt off at 500 ˚C for 10 hours with a slow ramping rate of 1 ˚C min^{-1}. The subsequent sintering was carried out for 2 hours on Pt foil at 1165 ˚C. The samples were buried by sacrificial powder of the same composition in a covered alumina crucible in order to inhibit the volatilization of potassium. The sintered samples were polished successively on a P1200 silicon carbide abrasive paper (Eco-Wet, KWH Mirka Ltd., Finland) using ethanol as the coolant, on a 3 μm grain-sized plate (MD Dur, Struers,

Denmark) with diamond suspension (DiaPro Mol B3, Struers, Denmark), and on a 1 μm grain-sized plate (MD Nap, Struers, Denmark) with diamond suspension (DiaPro Nap B1, Struers, Denmark). Such a process gave an average surface roughness of 50-60 nm. The final dimensions of the samples were 100-150 μm in thickness and 11.6-12.0 mm in diameter. The two surfaces of each sample were coated with 200 nm thick ITO (indium tin oxide) and 220 nm thick metal (20 nm Cr and 200 nm Au, Au on top) electrodes, respectively. Other compositions, i.e. KNN doped with different concentrations of BNNO, were fabricated by the same method presented above. More information about the sample fabrication can be found in reference.[11] The fabrication method of the reference BCZT sample can be found in reference.[26] However, the polishing and electrode deposition methods were the same as presented above.

Macroscopic characterization: The ferroelectric hysteresis loops (P-E loops) were measured with a ferroelectric test system (Precision LCII, Radiant Technologies, Inc., USA). The electrical resistivity was also measured together with the P-E loop measurements using the same equipment but with a DC field of 10 kV cm^{-1}. The pyroelectric current was obtained with a high-precision electrometer (B2985A, Keysight, USA) on a sample stage (LTS 350, Linkam Scientific Instruments, UK) which controlled the temperature. The photocurrent under halogen and deuterium light sources was recorded using the same electrometer. The same sample stage was also integrated with the ferroelectric test system for the measurement of P-E loops at different temperatures. The J-V curves and photocurrent with low bias electric field (±0.67 kV cm^{-1}) were measured with the 2450 SourceMeter (Keithley, USA). The poling process and the photocurrent recording with high bias electric field (10 kV cm^{-1}) were carried out with a poling station consisting of a voltage amplifier (Ultravolt, USA) and a data acquisition card (USB-6211, National Instruments, USA). Various light sources were involved: (1) Lasers (OBIS LX/LS series, Coherent, USA) with wavelength/maximum power/beam diameter at $1/e^2$ of 405 nm/50 mW/0.8±0.1 mm, 552 nm/20 mW/0.7±0.05 mm and 660 nm/100 mW/0.9±0.1 mm, respectively; (2) A fiber light source probe (DH-2000, Ocean Optics, USA) consisting of

deuterium and tungsten-halogen lamps with a beam size of 5 mm in diameter and with wavelength/power of 210-400 nm/217 µW and 300-1500 nm/295 µW, respectively; (3) A14 W white light energy saving fluorescent lamp (normal room light) which illuminated the entire sample surface with an intensity of ~12.5 mW cm^{-2}. This intensity was measured with a PM100D optical power and energy meter integrated with an S120C silicon photodiode detector (Thorlabs, Germany). The incident light was applied to the surfaces through a transparent (ITO) electrode.

Nanoscale measurements: The samples used for the nanoscale measurements were not coated with ITO electrodes. Only Cr-Au was deposited on one surface of each sample. The surface without an electrode was further polished to a surface roughness of 5-10 nm using a 0.25 µm diamond suspension (DiaPro Nap 1/4, Struers, Denmark). Samples were then investigated by AFM (Atomic Force Microscopy), PFM (Piezoresponse Force Microscopy) and KPFM (Kelvin-probe Force Microscopy). The nanoscale measurements were performed in the dark using a customized AIST-NT Smart SPM system. A Fianium Whitelase supercontinuum laser source was used to shine light with variable wavelength onto the sample. Initially, switching voltages were determined by electrical poling experiments. It was found that an AC bias of 0.4 V could cause partial switching of the sample. Therefore, an optimized AC bias of 0.2 V was applied between the conductive AFM tip (Platinum coated NSC35/PT probes from MikroMasch) and the bottom Cr-Au electrode for performing light induced temporal PFM measurements. KPFM measurements were performed in non-contact mode with a lift height of 10 nm. Initially, a smooth area was found and the AFM tip was maintained at a constant height of 10 nm from the surface. KPFM was performed with different wavelengths of the incident light at the same intensity.

Device demonstration: A poled KNBNNO sample (10 kV cm^{-1}, under 405 nm 50 mW laser, room temperature) was connected with a charged capacitor (100 µF, 18 V) and a resistive load (1 MΩ) in series. The voltage of the capacitor ($U_{capacitor}$) and the current of the entire circuit (I)

were recorded with the electrometer presented above. The resistance of the KNBNNO (R_{KNBNNO}) was measured with a multimeter (Model 115, Fluke, USA). The measurement setup is shown in Figure S9b-c in Supporting Information. The gross power (P_{gross}) on the resistive load (R_{load}) was calculated by $P_{gross} = I^2 \cdot R_{load}$. The power on the resistive load contributed by the capacitor ($P_{capacitor}$) was calculated by $P_{capacitor} = \left(\frac{U_{capacitor}}{R_{KNBNNO}+R_{load}}\right)^2 \cdot R_{load}$. The net power ($P_{net}$) on the resistive load is calculated by $P_{net} = P_{gross} - P_{capacitor}$.

Supporting Information
Supporting Information is available from the Wiley Online Library or from the author.

Acknowledgements
This work received funding from the European Union's Horizon 2020 research and innovation program under the Marie Sklodowska-Curie grant agreement number 705437. Author J.J. acknowledges the funding of the Academy of Finland (project numbers 267573, 273663 and 298409). The authors acknowledge the Centre of Microscopy and Nanotechnology of University of Oulu for the use of their facilities and for the fabrication of electrodes. Author J.S. acknowledges support by the Australian Research Council through Discovery grants. Y.B. fabricated the samples, carried out the macroscopic characterizations, analyzed the data and drafted the manuscript. G.V. implemented the nanoscale measurements and analyzed the data. All authors discussed the overall results, their relevance and conclusions. All authors co-wrote the paper.

Received: ((will be filled in by the editorial staff))
Revised: ((will be filled in by the editorial staff))
Published online: ((will be filled in by the editorial staff))

References

[1] V. M. Fridkin, *Photoferroelectrics*, Springer, Berlin **1979**.

[2] B. I. Sturman, V. M. Fridkin, *The photovoltaic and photorefractive effects in noncentrosymmetric materials*, Bordon and Breach, Amsterdam **1992**.

[3] V. M. Fridkin, , *IEEE Trans. Ultrason. Ferroelectr. Freq. Control.* **2013**, *60*(8), 1551-1555.

[4] J. E. Spanier, V. M. Fridkin, A. M. Rappe, A. R. Akbashev, A. Polemi, Y. Qi, Z. Gu, S. M. Young, C. J. Hawley, D. Imbrenda, G. Xiao, A. L. Bennett-Jackson, C. L. Johnson, , *Nat. Photonics.* **2016**, *10*(10), 688-688.

[5] C. Paillard, X. Bai, I. C. Infante, M. Guennou, G. Geneste, M. Alexe, J. Kreisel, B. Dkhil, , *Adv Mater.* **2016**, *28*(26), 5153-5168.

[6] R. Nechache, C. Harnagea, S. Li, L. Cardenas, W. Huang, J. Chakrabartty, F. Rosei, , *Nat. Photonics.* **2015**, *9*(1), 61-67.

[7] P. T. Chiu, D. C. Law, R. L. Woo, S. B. Singer, D. Bhusari, W. D. Hong, A. Zakaria, J. Boisvert, S. Mesropian, R. R. King, N. H. Karam, *35.8% space and 38.8% terrestrial 5J direct bonded cells*, IEEE, NEW YORK; 345 E 47TH ST, NEW YORK, NY 10017 USA **2014**.

[8] I. Grinberg, D. V. West, M. Torres, G. Gou, D. M. Stein, L. Wu, G. Chen, E. M. Gallo, A. R. Akbashev, P. K. Davies, J. E. Spanier, A. M. Rappe, , *Nature.* **2013**, *503*(7477), 509-+.

[9] Y. Bai, H. Jantunen, J. Juuti, , *Adv Mater.* **2018**.

[10] A. Polman, M. Knight, E. C. Garnett, B. Ehrler, W. C. Sinke, , *Science.* **2016**, *352*(6283), aad4424.

[11] Y. Bai, P. Tofel, J. Palosaari, H. Jantunen, J. Juuti, , *Adv Mater.* **2017**, *29*(29), 1700767.

[12] S. Yang, W. Fu, Z. Zhang, H. Chen, C. Li, , *J. Mater. Chem. A.* **2017**, *5*(23), 11462-11482.

[13] Y. Bai, T. Siponkoski, J. Perantie, H. Jantunen, J. Juuti, , *Appl. Phys. Lett.* **2017**, *110*(6), 063903.

[14] F. Li, D. Lin, Z. Chen, Z. Cheng, J. Wang, C. Li, Z. Xu, Q. Huang, X. Liao, L. Chen, T. R. Shrout, S. Zhang, , *Nat. Mater.* **2018**, *17*(4), 349-+.

[15] M. I. Asghar, J. Zhang, H. Wang, P. D. Lund, , *Renew. Sust. Energ. Rev.* **2017**, *77*, 131-146.

[16] D. Wang, M. Wright, N. K. Elumalai, A. Uddin, , *Solar Energy Mater. Solar Cells.* **2016**, *147*, 255-275.

[17] P. Wang, J. Zhao, L. Wei, Q. Zhu, S. Xie, J. Liu, X. Meng, J. Li, , *Nanoscale.* **2017**, *9*(11), 3806-3817.

[18] H. Borkar, M. Tomar, V. Gupta, R. S. Katiyar, J. F. Scott, A. Kumar, , *Mater. Res. Express.* **2017**, *4*(8), 086402.

[19] J. F. Scott, , *J. Phys. -Condes. Matter.* **2008**, *20*(2), 021001.

[20] H. Borkar, V. Rao, M. Tomar, V. Gupta, J. F. Scott, A. Kumar, , *RSC Adv.* **2017**, *7*(21), 12842-12855.

[21] F. Rubio-Marcos, D. A. Ochoa, A. Del Campo, M. A. Garcia, G. R. Castro, J. F. Fernandez, J. E. Garcia, , *Nat. Photonics.* **2018**, *12*(1), 29-+.

[22] D. Damjanovic, , *Rep. Prog. Phys.* **1998**, *61*(9), 1267-1324.

[23] K. Asadi, D. M. De Leeuw, B. De Boer, P. W. M. Blom, , *Nat. Mater.* **2008**, *7*(7), 547-550.

[24] G. F. A. Dibb, T. Kirchartz, D. Credgington, J. R. Durrant, J. Nelson, , *J. Phys. Chem. Lett.* **2011**, *2*(19), 2407-2411.

[25] M. Paire, A. Shams, L. Lombez, N. Pere-Laperne, S. Collin, J. Pelouard, J. Guillemoles, D. Lincot, , *Energy Environ. Sci.* **2011**, *4*(12), 4972-4977.

[26] Y. Bai, A. Matousek, P. Tofel, V. Bijalwan, B. Nan, H. Hughes, T. W. Button, , *J. Eur. Ceram. Soc.* **2015**, *35*(13), 3445-3456.

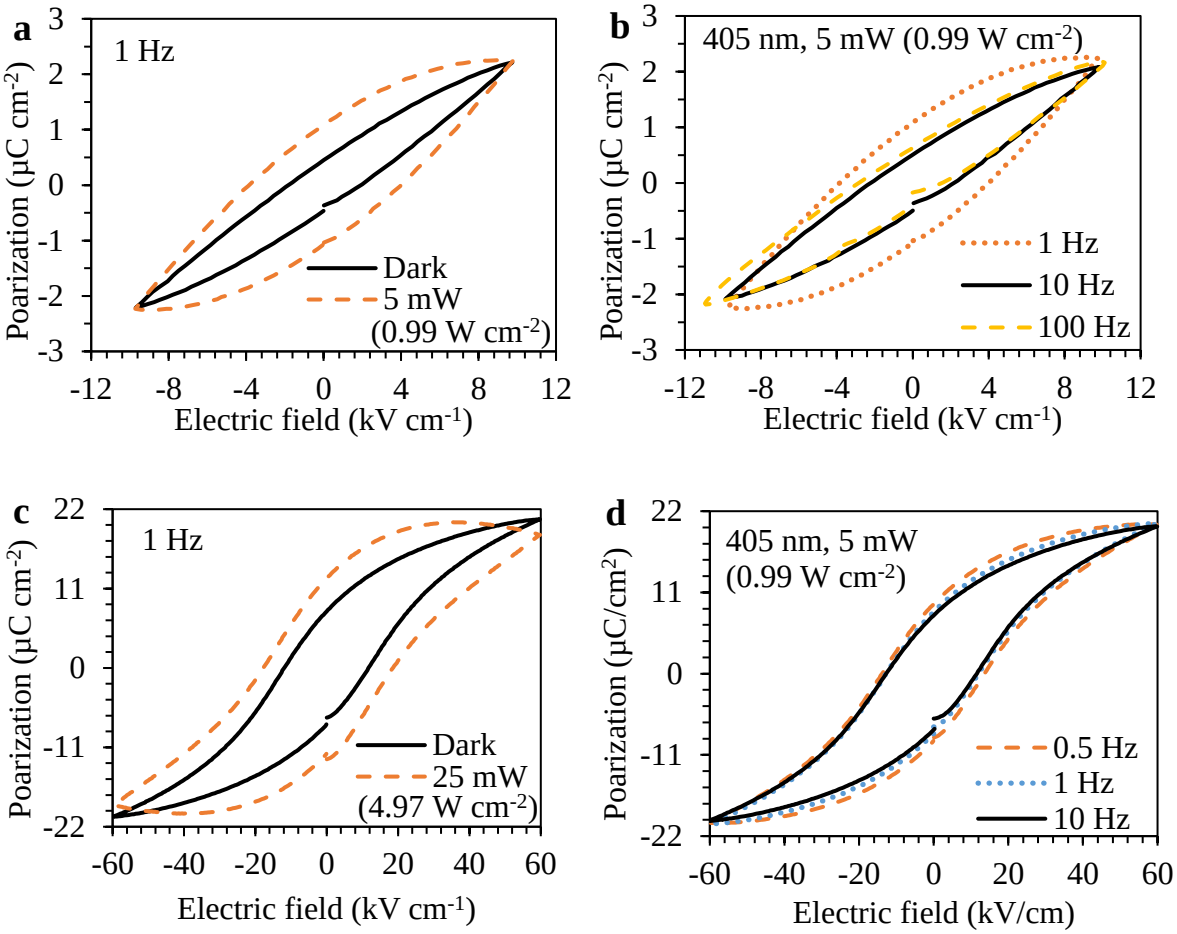

Figure 1. Ferroelectric enhancement under light illumination. P-E loops for the same KNBNNO sample measured in the dark, under illumination (405 nm laser) with different power inputs and at different frequencies of electric field. **a, c**, Unsaturated hysteresis loops with the maximum electric field smaller than the coercive force. **b, d,** Saturated hysteresis loops.

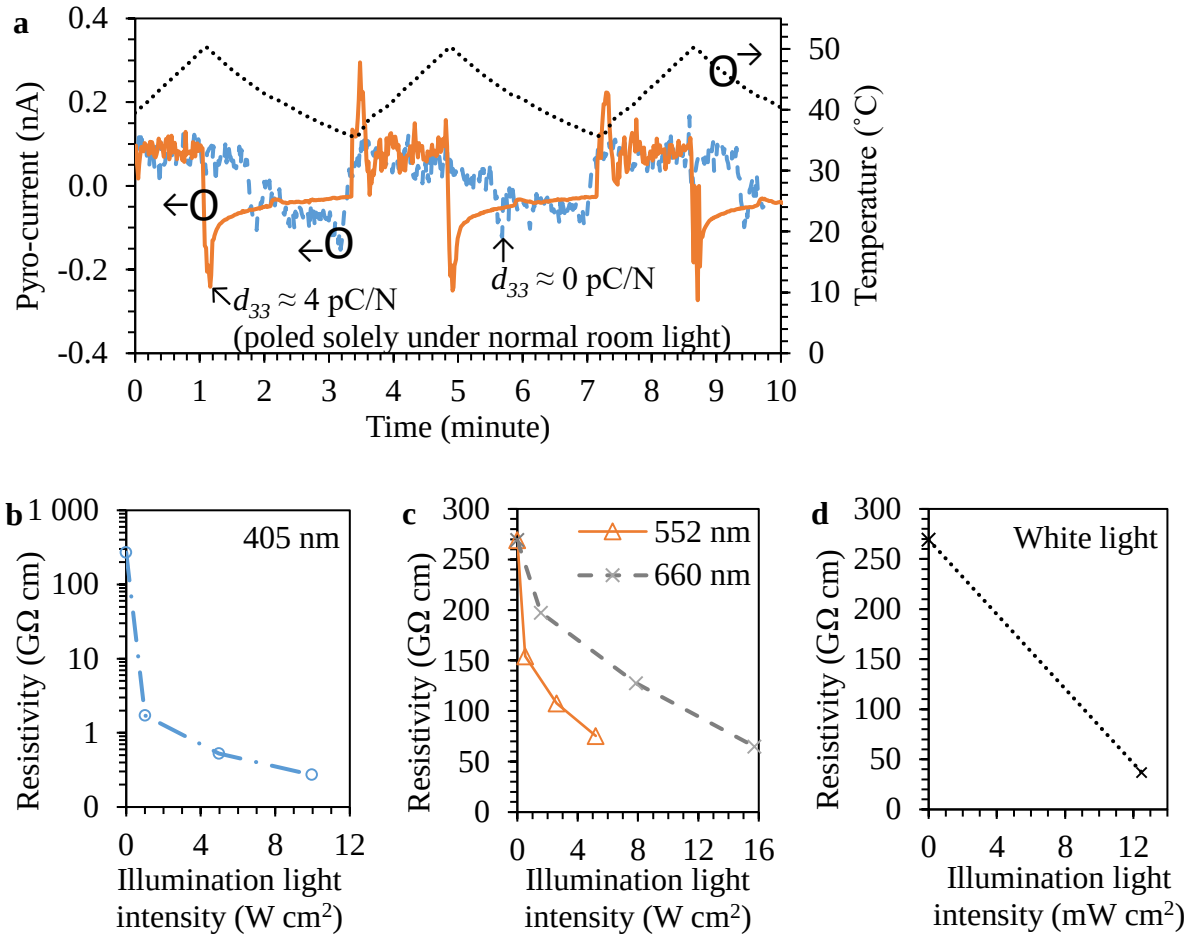

Figure 2. Interaction between illumination and electric, piezoelectric and pyroelectric properties. **a,** Dependence of pyroelectric current and temperature on time (pyroelectric response) measured in the dark for the same KNBNNO sample in unpoled status ($d_{33} \approx 0$ pC/N) and after poled only by applying white light ($d_{33} \approx 4$ pC/N). **b-d,** Dependence of resistivity on illumination power with different wavelengths for the same KNBNNO sample.

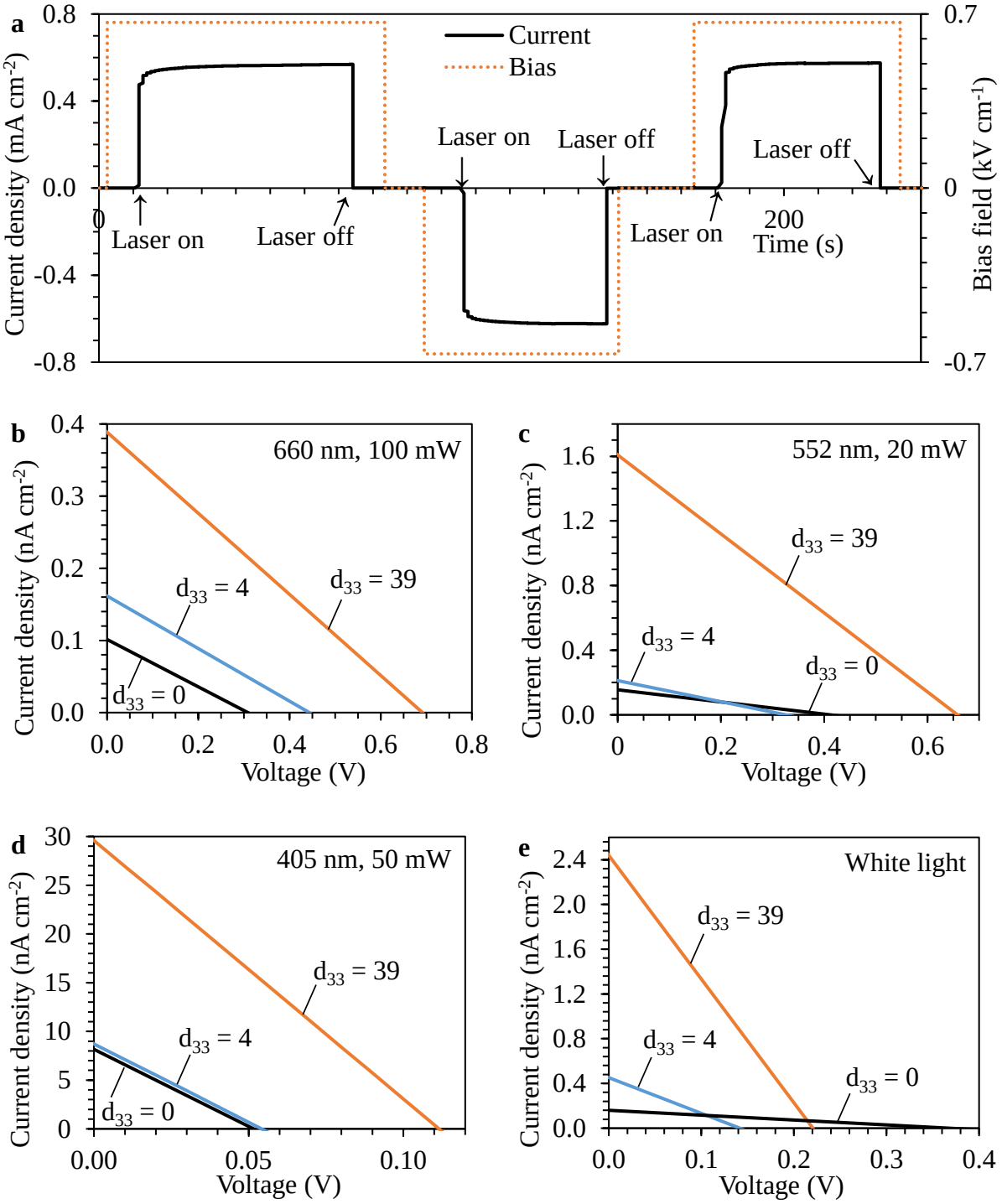

Figure 3. **Interaction and relationship between illumination, polarization, electric bias and photovoltaic performance. a,** The photocurrent response of the KNBNNO with DC bias and illumination (405 nm, 50 mW laser). **b-e,** I-V curves of the KNBNNO sample with different extents of domain alignment (indicated by d_{33} values with unit pC N^{-1}) and under different visible light sources. **b,** 660 nm, 100 mW laser. **c,** 552 nm, 20 mW laser. **d,** 405 nm, 50 mW laser. **e,** White light. d_{33} = 0, 4 and 39 means the sample was unpoled, poled solely by white

light and poled under 405 nm 50 mW laser with 10 kV cm^{-1} electric field at room temperature, respectively.

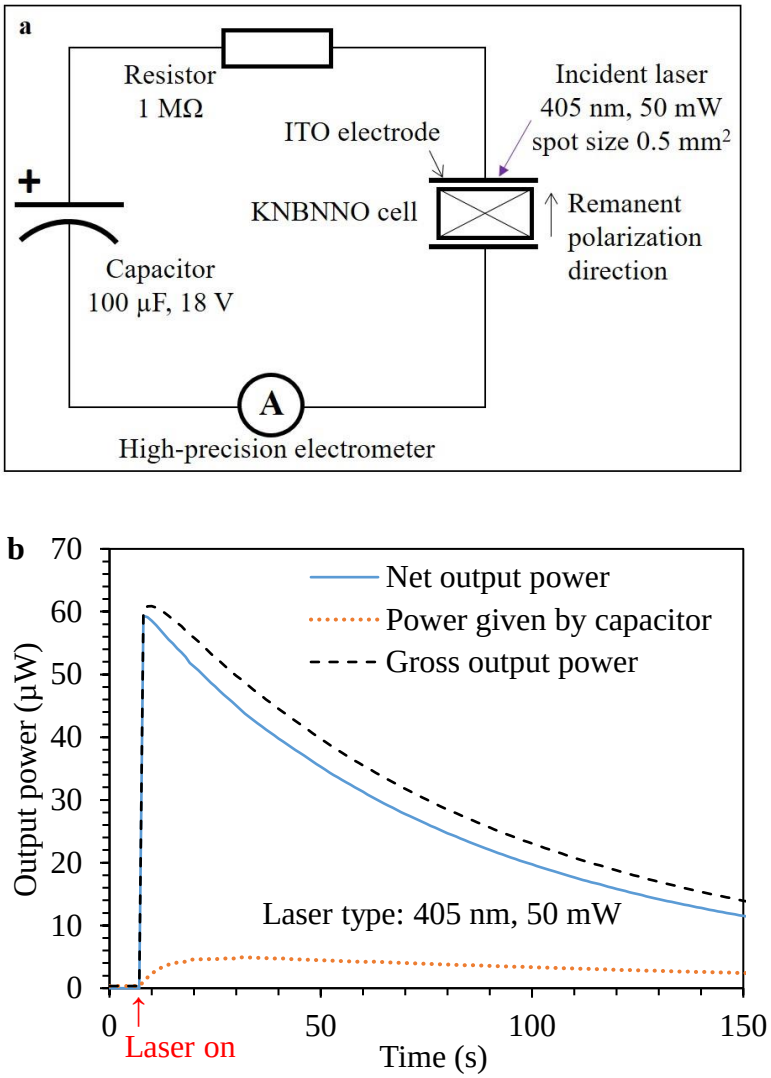

Figure 4. Demonstration of the photovoltaic output boost in a KNBNNO cell. a, The schematic of the energy harvesting circuit. **b,** The power given by the capacitor, gross power and net power on the 1 MΩ resistive load.

Table of content

Multi-source energy harvesting using monolithic photo-ferroelectric ceramics is an emerging and novel concept but still requiring a significantly improved photovoltaic energy conversion efficiency. Here, an approach has been proposed towards solving this issue. In addition, strong interaction between visible light and ferroelectric domain walls is observed, which was not possible previously using wide band gap photo-ferroelectrics.

Keywords

multi-source energy harvesting, photo-ferroelectric, ceramics, photovoltaic, efficiency boost

Y. Bai*, G. Vats, J. Seidel, H. Jantunen, J. Juuti

Title

Boosting photovoltaic output of ferroelectric ceramics by opto-electric control of domains

ToC figure